Journal of Chromatography A 1634 (2020) 461678

Contents lists available at ScienceDirect

Journal of Chromatography A

journal homepage: www.elsevier.com/locate/chroma

Short Communication

Importance of Particle Pore Size in Determining Retention and Selectivity in Reversed Phase Liquid Chromatography

Justin M. Godinho[a,*], Joseph A. Naese[b], Alexander E. Toler[b], Barry E. Boyes[a], Richard A. Henry[c], Joseph J. DeStefano[a], James P. Grinias[b,*]

[a] Advanced Materials Technology, Inc., 3521 Silverside Road, Wilmington, DE, 19810, USA
[b] Rowan University, Department of Chemistry & Biochemistry, 201 Mullica Hill Rd., Glassboro, NJ 08028, USA
[c] Independent Consultant, 983 Greenbriar Dr., State College, PA, 16801, USA

ARTICLE INFO

Article history:
Received 27 September 2020
Revised 30 October 2020
Accepted 1 November 2020
Available online 10 November 2020

Keywords:
Superficially Porous Particles
Pore Size
Size Exclusion Chromatography
Reversed Phase Chromatography

ABSTRACT

Column selection often centers on the identification of a stationary phase that increases resolution for a certain class of compounds. While gains in resolution are most affected by selectivity of the stationary phase or modifications of the mobile phase, enhancements can still be made with an intentional selection of the packing material's microstructure. Unrestricted mass transfer into the particle's porous structure minimizes band broadening associated with hindered access to stationary phase. Increased efficiency, especially when operating above the optimal flow rates, can be gained if the pore size is significantly larger than the solvated analyte. Less studied are the effects of reduced access to pores due to physical hindrance and its impact on retention. This article explores the relationship between pore size and reversed phase retention, and specifically looks at a series of particle architectures with reversed phase and size exclusion modes to study retention associated with access to stationary phase surface area.

1. Introduction

Method development in chromatography focuses on the desire to achieve optimal performance under a given set of experimental and instrumental conditions. One of the most important aspects of this process is column selection, including considerations for both the stationary phase that interacts with analytes and the architecture of support structures for the phase [1]. Improved chromatographic performance is often observed in idealized column structures, which include open tubes, ordered nonporous pillar arrays, and packed beds of nonporous spheres [2]. In these cases, very high performance has been demonstrated, but a lack of surface area prevents adequate sample (mass) load on a column for reliable detection post separation [3]. To increase surface area and ensure sufficient sample loadability, particles comprising chromatographic beds are typically highly porous [4].

When selecting a column support material for a given separation, a general requirement is that particle pore size should ensure analytes avoid restricted diffusion which results in poor chromatographic efficiency [5]. There are many "rules of thumb" for the minimum pore diameter-to-analyte diameter ratio, ranging from 4 to 10 [5,6]. However, a definitive guideline is difficult to establish as variables including the bonded phase and analyte size can be affected by separation conditions such as mobile phase and temperature [5,7,8].

The particles' porosity and mechanism of analyte diffusion into the porous surface is critical to the chromatographic process and largely the focus of chromatographic support study [9,10]. Larger pores reduce the obstruction of the analytes' movement thereby maintaining the analytes ability to diffuse efficiently. Too small, and the pores obstruct movement and cause lower chromatographic efficiency due to higher resistance to mass transfer. Theoretically, it would make sense to operate in the realm of very large pores, or even no pores, but these options reduce stationary phase surface area which can ultimately cause sample overloading [11]. For this reason, there is a direct compromise between efficiency and surface area. To address this compromise, and meet the analytical need for separation solutions of small and large molecules, various pore sizes are manufactured [12].

Although most research related to pore size in chromatographic particles focuses on efficiency, a less explored aspect of pore size is available retentive surface [13–16]. One recent comparison was made for very large molecules, myosin and the SigmaMab, on 1000 Å superficially porous particles (SPP) and 300 Å fully porous particles [17]. As the majority of the surface area of many chromato-

* Corresponding authors.
E-mail addresses: jgodinho@advanced-materials-tech.com (J.M. Godinho), grinias@rowan.edu (J.P. Grinias).

https://doi.org/10.1016/j.chroma.2020.461678
0021-9673/

graphic supports is buried deep within the particle, it stands to reason that limited access due to the size of analyte relative to pore size will reduce retention. In this communication, we explore this finding of restricted access to surface across highly similar superficially porous particle (SPP) architectures that differ in pore size and surface area, but have similar particle size and shell thickness. We demonstrate this phenomenon by tracking retention as a function of molecular weight in reversed phase modes and correlate it to the results of size exclusion experiments.

2. Experimental Conditions

2.1. Chemicals used

All solvents were HPLC grade or higher. Acetonitrile, trifluoroacetic acid, lorazepam, bombesin, insulin chain B oxidized, insulin and ribonuclease A were sourced from MilliporeSigma (St. Louis, MO). Trastuzumab was sourced as the injectable formulation (Herceptin, Roche), from a pharmaceutical supplier. The trastuzumab was reconstituted as recommended in the accompanying instructions, and stored as frozen concentrates that were thawed before use, then buffer exchanged by size exclusion into 50 mM ammonium bicarbonate buffer (pH 8.3). For SEC experiments, THF (unstabilized) was obtained from VWR Chemical (Radnor, PA) and toluene was from Pharmco-Aaper (Brookfield, CT). Polystyrene size standards between 1.9 kDa and 27.1 kDa were from Agilent Technologies (Wilmington, DE), between 50 kDa and 1.8 MDa were from Supelco (Bellefonte, PA), and the 2.8 MDa polystyrene standard was from Waters Corporation (Milford, MA).

2.2. Reversed phase experiments

Reversed phase LC experiments were conducted on a Shimadzu Nexera HPLC instrument with UV diode array detection (Columbia, MD). Detection wavelengths were 254 nm for small molecules and 210 nm for peptides and proteins. Chromatograms were processed with LabSolutions software (Shimadzu). Three 2.1 × 50 mm columns, a HALO 90 Å Phenyl-Hexyl, 2.7 µm, a HALO 160 Å Phenyl-Hexyl, 2.7 µm and a prototype phenyl-hexyl bonding on the HALO 1000 Å support, were used for reversed phase experiments (Advanced Materials Technology, Inc. Wilmington, DE). For van Deemter analysis, mobile phases compositions were proportioned by mass, premixed, and delivered to the column through a single pump at flow rates from 0.05 mL/min to 1.75 mL/min. Mobile phase compositions were determined experimentally to yield a retention factor (k') of 2 or greater for each individual analyte. Specific mobile phase percentages of acetonitrile in water (with 0.1% TFA) were as follows: lorazepam 30%, bombesin 21%, insulin chain B oxidized 28%, insulin 30% and ribonuclease A 22%. Experiments were conducted at 60 °C. For gradient experiments mobile phase A was water +0.1% TFA and mobile phase B was acetonitrile +0.1% TFA.

2.3. Size exclusion experiments

SEC experiments on HALO 90 Å HILIC (bare silica), HALO 160 Å bare silica column, and HALO 1000 Å bare silica columns (all 4.6 × 100 mm) were conducted on a HPLC system consisting of a Waters 600E Multisolvent Delivery System (Milford, MA), a Valco two-position, six-port injector (Houston, TX), and a Shimadzu SPD-10A UV/Vis detector (Columbia, MD) operated at 254 nm. Data was acquired at 20 Hz using a USB-6008 DAQ and in-house written LabView software (National Instruments, Austin, TX). All experiments to measure elution volume (calculated based on elution time) of toluene and polystyrene standards between 1.9 kDa and 2.8 MDa were conducted at 0.5 mL/min at ambient temperature with THF as the mobile phase.

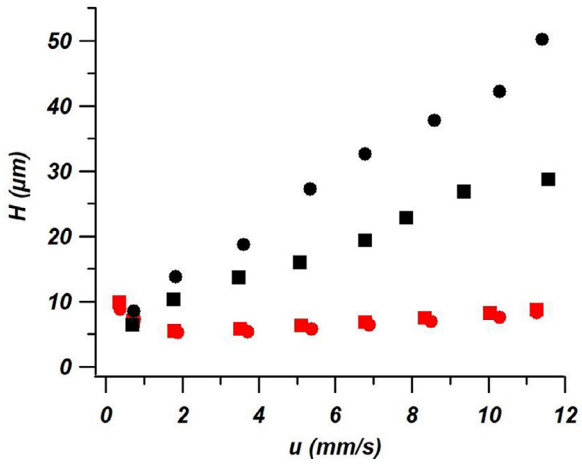

Fig. 1. Plate height vs. velocity plots for insulin (black) and lorazepam (red). Circles represent the results on the 90 Å material and squares are results from the 160 Å material.

3. Results and Discussion

Each of the HALO 90 Å, 160 Å and 1000 Å silica supports are physically similar with a 2.7 µm particle diameter, a 1.7 µm nonporous core and a 0.5 µm shell [17–20]. They differ in that each is synthesized to a unique shell porosity. With increasing shell porosity, the materials show reduced total surface area of 135, 90, and 25 m^2/gram, respectively. The following experiments control surface interaction as a variable by using HALO Phenyl-Hexyl bonding for reversed phase experiments and bare silica for size exclusion experiments.

Plate height was measured at varied flow rates by van Deemter type analysis of analytes on the 90 Å and 160 Å supports. Expected differences in performance as a function of molecular weight and pore size are shown in Fig. 1. For the small molecule lorazepam, 321 Da, the two columns perform nearly identically. This result eliminates column loading as a confounding variable. Comparison of insulin, 5777 Da, and lorazepam shows C-term increases due to the reduced diffusion coefficient of the larger molecule for both columns. Restricted access to the pores of the 90 Å material compared to the 160 Å material provided additional contribution to larger C-terms for the peptide hormone. This result is well understood and described in greater detail elsewhere [21–23].

The relative retention for these columns is consistent with trends observed in 300 – 1000 Å pore materials that were previously described by Wagner et. al. [17]. Plotted in Fig. 2A is a selection of chromatograms run at 0.5 mL/min, near the optimum flow rate for these SPP materials and column internal diameters. Notably, the retention order flips as the molecular weight of the analyte increases. For the smallest molecule, greater retention is seen on the 90 Å material as it can freely access the full intraparticle surface area in particles with both pore sizes. At 3496 Da, insulin chain B oxidized, the two peaks elute at nearly identical times, indicating similar access to the surface area in both columns and the beginning of restricted access to the intraparticle stationary phase, especially in the 90 Å column. Finally, insulin exhibits significantly greater retention on the 160 Å support as it has more access to intraparticle stationary phase surface area than in the 90 Å column.

Complete exclusion from the particles' porosity should return the ratio of retention factors to 1. As both materials have identical particle diameters, fully excluded analytes will experience the same total surface area of the packed spheres, specifically the sta-

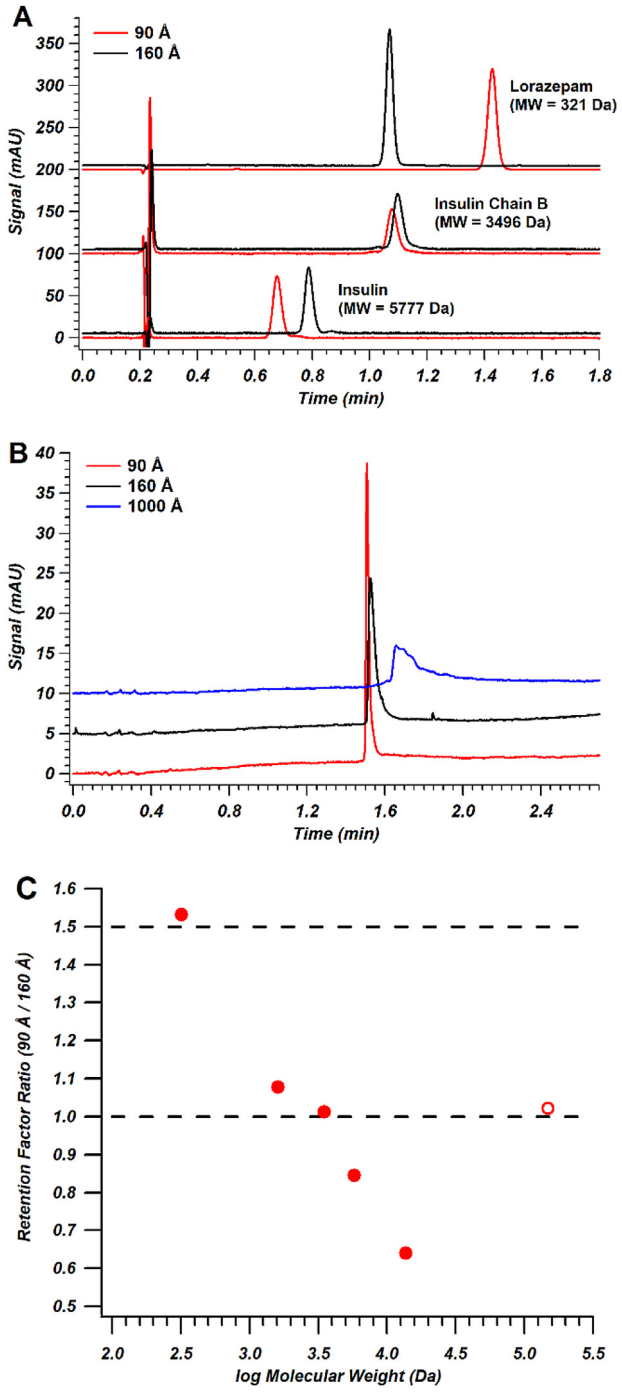

Fig. 2. Panel A, example isocratic chromatograms of lorazepam, insulin chain B oxidized, and insulin on 90 Å and 160 Å columns. Each is run at 0.5 mL/min. Panel B, gradient chromatograms run for trastuzumab. Gradient conditions were 20 to 50% B in 2.5 minutes at 60 °C and 0.5 mL/min. A plot of retention factor ratio as a function of log molecular weight is shown in Panel C. The dashed line at 1.5 represent the ratio of surface area between the materials 90 Å/160 Å. The dashed line at 1 represents the point of equal retention. Closed circles represent ratios of isocratic retention factor while the open circle represents the ratio of gradient retention factors.

tionary phase found on the outer particle surface. To observe this, we used the monoclonal antibody trastuzumab, 148 kDa, and modified our experiment to a gradient. Large molecules are difficult to separate under isocratic conditions due to their very steep S terms and it has been well documented that this value increases with the solute's molecular weight. The S term is the slope of the log k' vs ϕ (volume fraction of organic solvent in the mobile phase) plot [5]:

$$\log k' = log\ k_w - S\phi \quad (1)$$

Here, k_W is the retention factor in 100% water. Practically, a large S value results in very high retention and increased bandwidth due to longitudinal diffusion under retention conditions with weak mobile phases. Under higher strength isocratic conditions, retention is quickly eliminated. For this reason, we ran all isocratic experiments with premixed mobile phases. For the macromolecule trastuzumab, the S value is so large that we had to use a gradient for comparison, as shown in Fig. 2B. To interpret this data, we used the relative gradient retention values, k_g ,described in Equation 2 [24]:

$$k_g = \frac{t_r}{t_0} - 1 \quad (2)$$

The variables t_r and t_0 are the retention time and column dead time, respectively. As expected, trastuzumab yielded nearly identical k_g values for the 90 and 160 Å and a gradient retention factor ratio near 1. The peak on the 160 Å column is more tailed, likely due to some restricted partitioning into the pores that has been described previously with a "softball" model, which suggests molecules can access varying degrees of a particle's porosity and that this access depends on the molecules' size [25]. As an additional confirmation of principle, a prototype bonding of the Phenyl-Hexyl phase on our 1000 Å support was run for comparison. This material has approximately 19% of the total surface area of the 90 Å material and yet has greater retention under these conditions. Even in this unoptimized gradient for mAb separations, we begin to see features related to minor components, indicating non-excluded molecules are being separated. These minor components, thiol variants, have been well resolved under optimized reversed phase conditions on 1000 Å supports [26].

Fig. 2C plots the retention factor ratios and gradient retention factor ratios for a selection of test probes of varying molecular weights on the 90 Å and 160 Å columns. For this series of molecules, under denaturing conditions, a clear trend is seen as the retention factor ratio decreases from 1.5. The limit of 1.5 relates to the ratio of surface area between the 90 Å and 160 Å materials and is physically defined by the finite surface areas that a small molecule is able to freely sample. Small molecules behave as expected with a direct relationship to total available surface area. Medium size molecules, around 3000 Da, experience similar total surface area due to partial pore exclusion, or reduced access to the entirety of the pore size distribution. Molecules approaching 14,000 Da are mostly excluded from the 90 Å material, but have near full access to the available surface area on the 160 Å material. Very high molecular weight analytes, 150 kDa, are excluded from both the 90 Å and 160 Å materials resulting in equal retention on both columns. The true relationship between mass and size is complicated by experimental conditions [8]. As we do not have biophysical data for these molecules under these denaturing conditions, we have opted to plot results in terms of molecular weight instead of hydrodynamic volumes. For reference, models suggest a 3 kDa random coil would have a hydrodynamic radius of 45 Å, a 15 kDa random coil would be 100 Å in diameter, and a 150 kDa random coil would be 315 Å [5].

Size exclusion experiments were run to get a better understanding of the available pore volume and accessible surface using a simple model of bare silica and polystyrene standards in THF. Although this model is far from ideal for biomolecules and their reversed phase retention characteristics, it does give some insight into relative ranges of operation. Plots of log of the radius of gyration for polystyrene in THF as a function of retention volume are shown in Fig. 3. The useable SEC range for both materials was

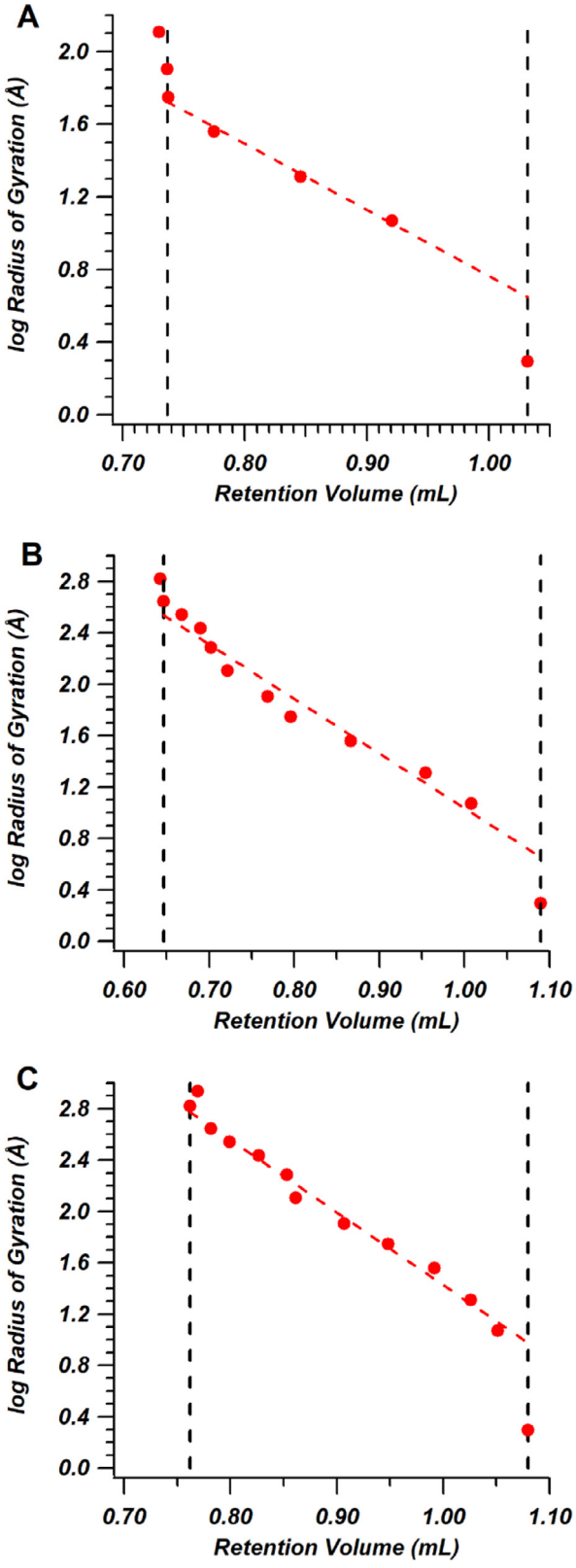

Fig. 3. Size exclusion data for the 90 Å (Panel A) 160 Å (Panel B) and 1000 Å (Panel C) columns. Dashed lines represent limits of total inclusion and full exclusion. Line of best fit for the linear region is shown in red.

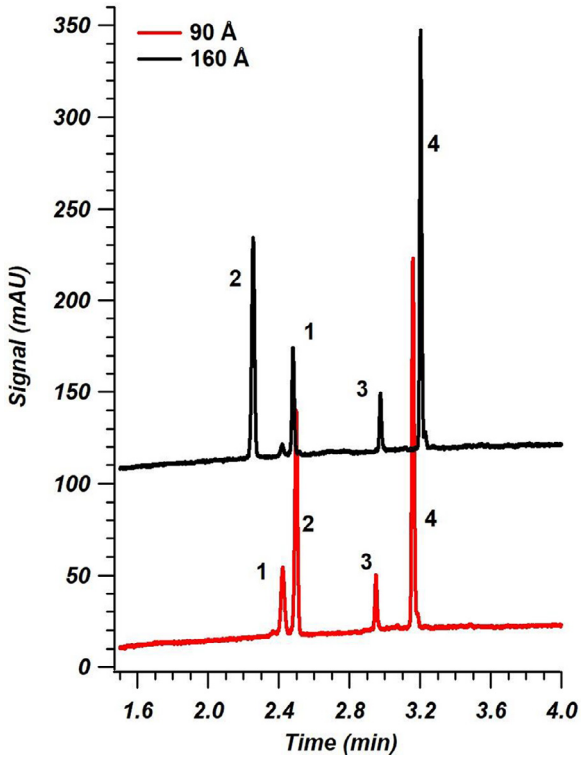

Fig. 4. Gradient chromatograms for the mix of ribonuclease A (1), lorazepam (2), insulin chain B oxidized (3) and insulin (4) on the 90 Å and 160 Å columns. Gradient conditions were 5 to 50% B in 5 minutes at 60 °C and 1.5 mL/min.

modeled with a linear fit between regions of full access and exclusion.

In practice, the development of an SEC protein separation begins with the selection of a column with a pore size that positions the band of interest near the middle of the fractionation range of the column, where $K_D = 0.5$ [27]. K_D, the distribution constant is defined in Equation 3 [27]:

$$K_D = (V_R - V_o)/V_P \quad (3)$$

Here V_R, V_O and V_P are elution volume, exclusion volume, and pore volume respectively. Using this rule of thumb for our columns, the point at which $K_D = 0.5$ for the 90 Å material is 3100 Da, the 160 Å material is 19.9 kDa and the 1000 Å is 48 kDa. These values approximate ranges where we could expect 50% access to the pore volume and about the same access to surface area of the particle. However, because the pore size distribution in these materials is wide and larger molecular weight solutes are flexible, no hard cut-off of solute molecular weight exists and efficient separations can be achieved with each of these materials in gradient modes. Examples of this can be seen throughout the literature for very large pore monoclonal antibody separations [17,26,28,29].These results do suggest that even more gains in potential retention manipulation, selectivity, and resolution could be achieved with even larger pores.

Leveraging exclusion-based retention with analyte mixes of significantly different molecular weights could be an important tool for modifying selectivity that is currently underutilized. For example, Fig. 4 shows the gradient elution of a mixture of 4 compounds. Shifts in retention are related to analyte MW and access to available surface area. Peaks 1 and 4, ribonuclease A and insulin, gain retention on the 160 Å column. Peak 2, lorazepam, has less retention on the lower surface area 160 Å column. Peak 3, insulin Chain B oxidized, does not shift and elutes at 2.949 (90 Å) and 2.976 (160 Å) minutes. The pore size difference in the two columns results in

a change in elution sequence for lorazepam and insulin chain B oxidized peaks. In practice, relative retention shifts could be increased by shallower gradients. An example of exploiting this size-exclusion effect in reversed phase mode was recently described by Huang *et al*., in which a method developed to determine chelating agents' concentrations by excluding the larger mAb from the already formulated sample in the void volume and reducing the need for longer sample preparation steps [30]. The results from Fig. 4 demonstrate that these retention shifts can be more subtle in the range between completely unrestricted access to intraparticle surface area and complete exclusion from pores, providing an additional method development parameter for peptide and protein separations.

4. Conclusions

Although reversed phase retention of small molecules has been well described, a subtle phenomenon relating reversed phase retention, pore size, analyte size and available surface area has received less attention. Modern particles prepared from sols by a process that yields highly reproducible porosity could restore interest in the use of pores as a retention variable when sample components vary significantly in MW. Retention shifts based on analyte size were identified using identical bonded phases on highly similar particle architectures that only differ in pore size and surface area. Our results with current particles suggest pore size could play a more significant role in method development by giving protocols another variable of manipulation. Given the current trend towards biologics in the pharmaceutical industry, we believe this phenomenon could be very powerful to manipulate analyte selectivity, especially in samples of diverse molecular weights.

We also present evidence for a continued drive towards even larger pore materials. As detection schemes and instrumentation develop to handle even smaller mass loads, the chromatography column will be given more room to operate in highly efficient, low surface area configurations. We expect this could manifest through increasing pore diameter within the limits of particle stability and eventually routine application of nonporous particles or open tubular separations. These regimes of operation are however fraught with experimental challenges that will need to be addressed including sample handling, relative dynamic range of sample concentrations, and sensitive detection schemes. Given that resolution is strongly a function of surface driven selectivity, a balance will be required for the successful application of next generation chromatographic materials.

Declaration of Competing Interest

JMG, BEB and JJD are employed by a company that manufactures some of the materials referenced in this article.

CRediT authorship contribution statement

Justin M. Godinho: Conceptualization, Methodology, Investigation, Writing - original draft, Writing - review & editing, Visualization. **Joseph A. Naese:** Investigation. **Alexander E. Toler:** Investigation. **Barry E. Boyes:** Conceptualization, Writing - review & editing, Funding acquisition. **Richard A. Henry:** Conceptualization, Writing - review & editing. **Joseph J. DeStefano:** Conceptualization, Writing - review & editing. **James P. Grinias:** Conceptualization, Writing - review & editing, Visualization, Funding acquisition.

Acknowledgements

Acknowledgment is made to the Donors of the American Chemical Society Petroleum Research Fund for partial support of this research, and the NIH Award R44 GM116224 (BEB). The views and opinions expressed in this publication do not reflect endorsement by, or opinions of, the sources of financial support of this research.

References

[1] L.R. Snyder, J.J. Kirkland, J.L. Glajch, Practical HPLC Method Development, 2nd ed., John Wiley & Sons, Hoboken, NJ, 1997 https://doi.org/10.1002/9781118592014.
[2] G. Desmet, S. Eeltink, Fundamentals for LC Miniaturization, Anal. Chem. 85 (2013) 543–556 https://doi.org/10.1021/ac303317c.
[3] G. Guiochon, The limits of the separation power of unidimensional column liquid chromatography, J. Chromatogr. A. 1126 (2006) 6–49 https://doi.org/10.1016/j.chroma.2006.07.032.
[4] J.S. Mellors, J.W. Jorgenson, Use of 1.5-µm porous ethyl-bridged hybrid particles as a stationary-phase support for reversed-phase ultrahigh-pressure liquid chromatography, Anal. Chem. 76 (2004) 5441–5450 https://doi.org/10.1021/ac049643d.
[5] L.R. Snyder, J.J. Kirkland, J.W. Dolan, Introduction to Modern Liquid Chromatography, 3rd ed., John Wiley & Sons, Inc., Hoboken, NJ, USA, 2010 https://doi.org/10.1002/9780470508183.
[6] A.F. Bergold, A.J. Muller, D.A. Hanggi, P.W. Carr, HIGH-PERFORMANCE AFFINITY CHROMATOGRAPHY, in: C.B.T.-H.-P.L.C. Horváth (Ed.), High Perform. Liq. Chromatogr. Adv. Perspect., Academic Press, 1988, pp. 95–209. https://doi.org/10.1016/B978-0-12-312205-6.50006-0.
[7] M.T.W. Hearn, M.I. Aguilar, High-performance liquid chromatography of amino acids, peptides and proteins. LXXIII. Investigations on the relationships between molecular structure, retention and band-broadening properties of polypeptides separated by reversed-phase high-performance liquid chromatography-quid chromatography, J. Chromatogr. A. 397 (1987) 47–70 https://doi.org/10.1016/S0021-9673(01)84989-X.
[8] K.D. Nugent, W.G. Burton, T.K. Slattery, B.F. Johnson, L.R. Snyder, Separation of proteins by reversed-phase high-performance liquid chromatography. II. Optimizing sample pretreatment and mobile phase conditions, J. Chromatogr. A. 443 (1988) 381–397 https://doi.org/10.1016/S0021-9673(00)94809-X.
[9] F. Gritti, G. Guiochon, Mass transfer kinetics, band broadening and column efficiency, J. Chromatogr. A. 1221 (2012) 2–40 https://doi.org/10.1016/j.chroma.2011.04.058.
[10] J. Urban, P. Jandera, Z. Kučerová, M.A. van Straten, H.A. Claessens, A study of the effects of column porosity on gradient separations of proteins, J. Chromatogr. A. 1167 (2007) 63–75 https://doi.org/10.1016/j.chroma.2007.08.027.
[11] F. Gritti, G. Guiochon, Comparison between the loading capacities of columns packed with partially and totally porous fine particles. What is the effective surface area available for adsorption? J. Chromatogr. A. 1176 (2007) 107–122 https://doi.org/10.1016/j.chroma.2007.10.076.
[12] R.A. Henry, S.A. Schuster, How to Avoid Size Mismatch Between Solutes and Column Pores for Optimum HPLC Performance Development, Am. Lab. 49 (2017) 22–27.
[13] J. Klein, K. Treichel, Superposition of permeation and adsorption effects in liquid chromatography, Chromatographia 10 (1977) 604–610 https://doi.org/10.1007/BF02265039.
[14] K.K. Unger, Silica as packing in size-exclusion chromatography, in: J. Chromatogr. Libr. Porous Silica, Elsevier, Amsterdam, Netherlands, 1979, pp. 271–289. https://doi.org/10.1016/S0301-4770(08)60813-1.
[15] F. Eisenbeiss, S. Ehlerding, High Speed Separations of Oligomers and Polymers by HPLC on Analytical and Preparative Scale, Kontakte 1 (1978) 22–29.
[16] H. Engelhardt, D. Mathes, High-performance exclusion chromatography of water-soluble polymers with chemically bonded stationary phases, J. Chromatogr. A. 185 (1979) 305–319 https://doi.org/10.1016/S0021-9673(00)85611-3.
[17] B.M. Wagner, S.A. Schuster, B.E. Boyes, T.J. Shields, W.L. Miles, M.J. Haynes, R.E. Moran, J.J. Kirkland, M.R. Schure, Superficially porous particles with 1000 Å pores for large biomolecule high performance liquid chromatography and polymer size exclusion chromatography, J. Chromatogr. A. 1489 (2017) 75–85 https://doi.org/10.1016/j.chroma.2017.01.082.
[18] J.J. DeStefano, T.J. Langlois, J.J. Kirkland, Characteristics of superficially-porous silica particles for fast HPLC: some performance comparisons with sub-2-micron particles., J. Chromatogr. Sci. 46 (2008) 254–260 https://doi.org/10.1093/chromsci/46.3.254.
[19] S.A. Schuster, B.M. Wagner, B.E. Boyes, J.J. Kirkland, Wider pore superficially porous particles for peptide separations by hplc, J. Chromatogr. Sci. 48 (2010) 566–571 https://doi.org/10.1093/chromsci/48.7.566.
[20] S.A. Schuster, B.E. Boyes, B.M. Wagner, J.J. Kirkland, Fast high performance liquid chromatography separations for proteomic applications using Fused-Core® silica particles, J. Chromatogr. A. 1228 (2012) 232–241 https://doi.org/10.1016/j.chroma.2011.07.082.
[21] J.C. Giddings, Dynamics of chromatography, Part 1: Principles and Theory, Marcel Dekker, New York, NY, 1965.
[22] F. Gritti, G. Guiochon, The quantitative impact of the mesopore size on the mass transfer mechanism of the new 1.9 μm fully porous Titan-C18 particles. I: Analysis of small molecules, J. Chromatogr. A. 1384 (2015) 76–87 https://doi.org/10.1016/j.chroma.2015.01.047.
[23] F. Gritti, G. Guiochon, The quantitative impact of the mesopore size on the mass transfer mechanism of the new 1.9μm fully porous Titan-C18 particles II - Analysis of biomolecules, J. Chromatogr. A. 1392 (2015) 10–19 https://doi.org/10.1016/j.chroma.2015.02.075.

[24] U.D. Neue, Theory of peak capacity in gradient elution, J, Chromatogr. A. 1079 (2005) 153–161 https://doi.org/10.1016/j.chroma.2005.03.008.
[25] J.P. Larmann, J.J. DeStefano, A.P. Goldberg, R.W. Stout, L.R. Snyder, M.A. Stadalius, Separation of macromolecules by reversed-phase high-performance liquid chromatography. Pore-size and surface-area effects for polystyrene samples of varying molecular weight, J. Chromatogr. A. 255 (1983) 163–189 https://doi.org/10.1016/S0021-9673(01)88282-0.
[26] B. Wei, B. Zhang, B. Boyes, Y.T. Zhang, Reversed-phase chromatography with large pore superficially porous particles for high throughput immunoglobulin G2 disulfide isoform separation, J. Chromatogr. A. 1526 (2017) 104–111 https://doi.org/10.1016/j.chroma.2017.10.040.
[27] B.F.D. Ghrist, M.A. Stadalius, L.R. Snyder, Predicting bandwidth in the high-performance liquid chromatographic separation of large biomolecules. I. Size-exclusion studies and the role of solute stokes diameter versus particle pore diameter, J. Chromatogr. A. 387 (1987) 1–19 https://doi.org/10.1016/S0021-9673(01)94510-8.
[28] B. Bobály, J.L. Veuthey, D. Guillarme, S. Fekete, New developments and possibilities of wide-pore superficially porous particle technology applied for the liquid chromatographic analysis of therapeutic proteins, J. Pharm. Biomed. Anal. 158 (2018) 225–235 https://doi.org/10.1016/j.jpba.2018.06.006.
[29] D.V. McCalley, D. Guillarme, Evaluation of additives on reversed-phase chromatography of monoclonal antibodies using a 1000 Å stationary phase, J. Chromatogr. A. 1610 (2020) 460562 https://doi.org/10.1016/j.chroma.2019.460562.
[30] J.Z. Huang, K. Liao, G. Wang, T. Haby, M.S. Bolgar, Exploitation of the size-exclusion effect of reversed-phase high performance liquid chromatography for the direct analysis of diethylene triamine pentaacetic acid in therapeutic monoclonal antibody formulations, J. Chromatogr. A. 1455 (2016) 140–146 https://doi.org/10.1016/j.chroma.2016.05.087.